IRAQI JOURNAL OF MATERIALS
Volume (4) Issue (2) April-June 2025, pp. 81-88

Indium Nitride Nanostructures Synthesized by Pulsed Laser Ablation in Hydroxide Solution

Alireza M. Rahmatzadeh, Farhad A. Bahrooz

Department of Materials Engineering, Shahid Shamsipour Institute of Technology, Tehran, IRAN

Abstract
In this work, indium nitride (InN) nanoparticles were prepared by pulsed laser ablation (PLAL) by irradiation of In target immersed in NH_4OH solution. The crystalline structure of the prepared nanoparticles was found to be wurtzite with tending to much more crystallization when higher laser energy is used in preparation process. These nanoparticles show large aggregations to form reef-like structures. Using higher laser energy to prepare them has resulted in much more aggregations. No indium clusters were observed in the surface morphology of the prepared samples, indicating a complete reaction of indium with nitrogen. All functional groups constituting the indium nitride molecule were found in the prepared samples with no trace belonging to other materials, which reflects the high structural purity of the prepared nanoparticles. The absorbance of the prepared nanoparticles was found to depend on the laser energy used to prepare them, which determines the volume concentration of these nanoparticles, and hence the density of the solution to be measured.

Keywords: Indium nitride; Laser ablation; Nanostructures; Structural characteristics
Received: 01 February 2025; **Revised:** 04 March 2025; **Accepted:** 18 March 2025; **Published:** 1 April 2025

1. Introduction

Nanostructures, including particles, wires, and tubes, have garnered significant research attention due to their distinctive applications in microscopic physics, chemistry, and the development of nanoscale devices [1,2]. Consequently, numerous self-assembly and synthesis methods have been developed in recent years to create various nanometer-sized building blocks [3]. Among these, laser ablation of solids in liquids has emerged as a unique technique for synthesizing nanostructures [4,5]. This method has led to a surge of studies exploring nanostructure formation via laser ablation in recent years [6]. Laser ablation, a materials-processing technique, has been known since the invention of the laser in 1960, originally developed following the creation of the ruby laser [7-9]. Over the past decade, extensive experimental and theoretical research has focused on this technique. Laser ablation in liquids, specifically for solid targets, is a relatively recent approach introduced in 1993 [10]. This top-down fabrication method enables the creation of nanostructures with diverse compositions and morphologies [11]. Various materials, including metals, alloys, oxides, carbides, and hydroxides, can serve as targets, producing structures such as nanoparticles, nanocubes, nanorods, and nanocomposites [12-15].

The process of laser ablation is highly complex, involving the ejection of material from a solid surface induced by the interaction of short (~nanoseconds to picoseconds), intense (~10^6 to 10^{14} W/cm^2) laser pulses [16]. This process can occur in vacuum, gas, or liquid environments, provided the gas or liquid does not significantly reduce the laser's energy or light intensity at the solid's surface [17]. In liquid-based laser ablation, a high-power laser beam is focused on the surface of a solid target submerged in a specific liquid [18]. The laser's interaction with the target surface vaporizes it, generating an ablation plume containing high-energy species like atoms, ions, and clusters [19]. These ejected species interact with molecules in the surrounding liquid, forming new compounds that include elements from both the target and the liquid [20]. This technique benefits from the combination of nanosecond laser pulses, extreme temperatures, and pressures within the reaction zone, which can reach several thousand Kelvin and tens of GPa [21]. These conditions create a high-temperature, high-pressure, and high-density environment, providing a "brute force" approach to synthesizing novel materials that were previously unattainable using more conventional and moderate methods [22,23].

The laser ablation in liquid (LAL) process begins with the interaction of laser light with the surface of a solid target [24]. This triggers chemical reactions between the particles in the resulting plume and the molecules of the surrounding liquid. These collisions lead to the formation of new compounds, typically nanoparticles composed of atoms from both the target material and the liquid [25]. These nanoparticles become suspended in the liquid, forming a colloidal solution. As the nanoparticles aggregate, additional

reactions may occur due to the presence of laser radiation, which can further alter the composition, size, and morphology of the final product [26].

The benefits of the laser ablation in liquid technique are as follows. Laser pulses can reach the surface of a submerged target as long as the liquid is transparent to the laser light [27]. The method is versatile and can be applied to any type of target material. The ablated species, such as atoms and ions, are often in highly excited states, allowing them to emit light [28]. The liquid confines the ablated species to a small region, resulting in high pressure and density during the initial stages of ablation. The technique is cost-effective and straightforward, as it eliminates the need for vacuum equipment [29]. Nanoparticles are easily collected after synthesis, as they are stored in the liquid as a colloidal solution. The ablated material can serve as a precursor for chemical reactions, particularly in nanoparticle formation [30]. The expansion of particles ejected from the target is significantly limited due to the confinement effect of the surrounding liquid. A cavitation bubble forms after the plasma disappears, accompanied by optical emission [31].

Despite the distinct advantages of liquid-phase laser ablation, it has certain limitations. One major drawback is the inability to effectively control plasma properties [32]. The nanoparticles produced through this method often exhibit a broad size distribution, which is attributed to the agglomeration of nanoclusters and the potential release of larger target fragments during the ablation process. Additionally, a relatively low product yield is a significant disadvantage of this technique [33]. Indium nitride (InN) is a binary III-V semiconductor composed of indium (In) and nitrogen (N). It crystallizes in a hexagonal wurtzite structure under normal conditions, although a metastable cubic phase can also exist under specific conditions [34]. The material has a relatively low bandgap energy of approximately 0.7 eV, making it a promising candidate for infrared and high-speed electronic applications. InN exhibits high electron mobility, typically exceeding 2000 $cm^2/V \cdot s$ at room temperature, which contributes to its potential for high-performance electronic devices [35]. Fig. (1) Bulk crystal structure from wurtzite indium nitride (InN) viewed along the c-axis (a) and laterally (b), as obtained from full relaxation of ionic positions and lattice parameters. Level of theory: 800 eV/9x9x9 k-points.

The physical properties of InN include a high melting point (around 1200 °C) and strong piezoelectric and pyroelectric effects due to its crystal structure. It also possesses a high thermal conductivity, making it suitable for high-temperature applications [36]. Chemically, indium nitride is relatively stable but reacts with oxygen at elevated temperatures, forming an oxide layer. It also exhibits a strong affinity for hydrogen, which plays a role in its synthesis and properties [37].

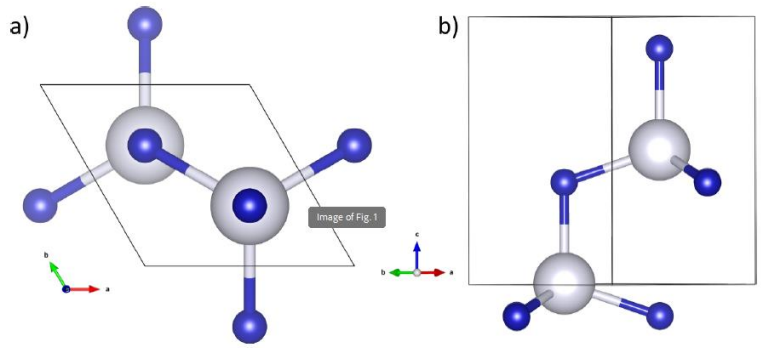

Fig. (1) Bulk crystal structure from wurtzite indium nitride (InN) viewed along the c-axis (a) and laterally (b), as obtained from full relaxation of ionic positions and lattice parameters. Level of theory: 800 eV/9x9x9 k-points [38]

Several methods have been developed to synthesize indium nitride, each with its advantages and limitations. Molecular Beam Epitaxy (MBE) is a widely used technique for producing high-purity, single-crystalline InN films [38,39]. It involves the reaction of indium and nitrogen sources, such as ammonia or nitrogen plasma, in a vacuum environment [40]. The low growth temperature and high control over the deposition process make MBE ideal for fabricating high-quality InN layers [41]. Metal-Organic Chemical Vapor Deposition (MOCVD) utilizes organometallic precursors, such as trimethylindium, and ammonia as the nitrogen source [42]. The reaction occurs at elevated temperatures, allowing for the deposition of InN on various substrates. This method is scalable and suitable for industrial applications. Reactive sputtering technique involves bombarding an indium target with ions in a nitrogen-containing plasma [4]. This method can produce polycrystalline InN films but often requires post-deposition annealing to improve crystallinity [43]. Hydrothermal synthesis involves the reaction of indium salts with

nitrogen sources, such as ammonia, under high pressure and temperature in an aqueous environment. It is suitable for synthesizing InN nanoparticles [44].

Indium nitride has garnered significant attention due to its unique properties, enabling a wide range of applications. The low bandgap and high electron mobility make InN an ideal material for infrared photodetectors, light-emitting diodes (LEDs), and laser diodes [45-48]. Its ability to cover a broad spectrum of wavelengths enhances its utility in optoelectronic devices. The high electron mobility and thermal conductivity of InN are advantageous for fabricating high-frequency transistors and other electronic components used in wireless communication and radar systems [49]. Tunable bandgap of InN enables its use in multi-junction solar cells, where it can capture infrared radiation to improve energy conversion efficiency [50]. InN-based sensors exhibit high sensitivity to gases like hydrogen due to their strong interaction with the material's surface, making them suitable for environmental monitoring and industrial applications [60].

The future of indium nitride research and development holds promising possibilities. Efforts are ongoing to overcome challenges such as controlling defect densities, improving crystal quality, and enhancing material stability [61]. Advances in nanotechnology may enable the synthesis of InN nanostructures with tailored properties, opening doors to novel applications in quantum computing and nanoscale electronics [2]. Moreover, integrating InN with other III-V semiconductors in heterostructures and devices could revolutionize the field of optoelectronics and high-power electronics [33]. As sustainable technologies gain momentum, InN's potential role in next-generation solar cells and hydrogen sensing for clean energy applications is likely to expand significantly [64]. Indium nitride's remarkable properties and versatile applications position it as a material of immense scientific and technological interest. Continued research and innovation will be key to unlocking its full potential in diverse fields.

2. Experimental Work

The experimental setup shown in Fig. (2) for the laser ablation of an indium target submerged in a 20% NH_4OH solution includes a HUAFEI Nd:YAG laser system operating at 1064 nm, with maximum pulse energy of 1000 mJ, pulse width of 10 ns, and repetition rate of 1 Hz. A lens with a focal length of 15 cm was used to focus the laser beam to increase the laser fluence. A pure (0.999) indium target supplied from HIMEDIA measuring 5×10×1 mm^3 was used to produce indium nitride (InN) nanoparticles. The ablation process was conducted at room temperature for durations of 5, 10, and 15 minutes using different laser energies (40, 60, 80, 100 and 120 mJ). The laser ablation experiments involving the indium target in NH_4OH solution were carried out within this sealed cell.

The x-ray diffraction (XRD) patterns of the prepared samples were recorded using a Shimadzu 6000 X-ray diffractometer. The field-emission scanning electron microscopy (FE-SEM) was performed on the prepared samples using an FEI Inspect f50 FE-SEM instrument. A Shimadzu 8000S was used to record the Fourier-transform infrared (FTIR) spectra of the prepared samples. The UV-visible spectrophotometry was performed on the prepared samples using a Perkin-Elmer spectrophotometer in the spectral range of 200-1000nm.

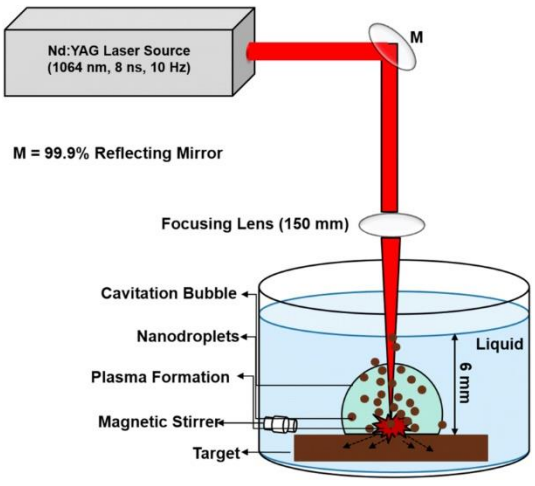

Fig. (2) The experimental setup of the PLAL to prepare InN nanoparticles

3. Results and Discussion

Figure (3) shows the XRD patterns of the InN nanoparticles prepared in this work at different laser energies. All samples show polycrystalline structures with distinct diffraction peaks at diffraction angles of 29.13°, 31.31°, 33.14°, 51.07°, and 60.89° those corresponding to the crystal orientations of (100), (002), (101), (110), and (112), respectively. These diffraction peaks confirm the formation of wurtzite InN structure. Some other peaks were not seen in the sample prepared using 40mJ laser energy while they appeared in the samples prepared at higher laser energies. These peaks are seen at diffraction angles of 43.35° (102), 56.90° (103), and 63.11° (201). These changes can be attributed to the increment of the crystallite size as the crystallite gained more kinetic energy at higher temperature. These results were compared to the JCPDS card no. 021450. The lattice parameters *a* and *c* for prepared nanoparticles were 3.53-3.54 Å and 5.70-5.73 Å, respectively.

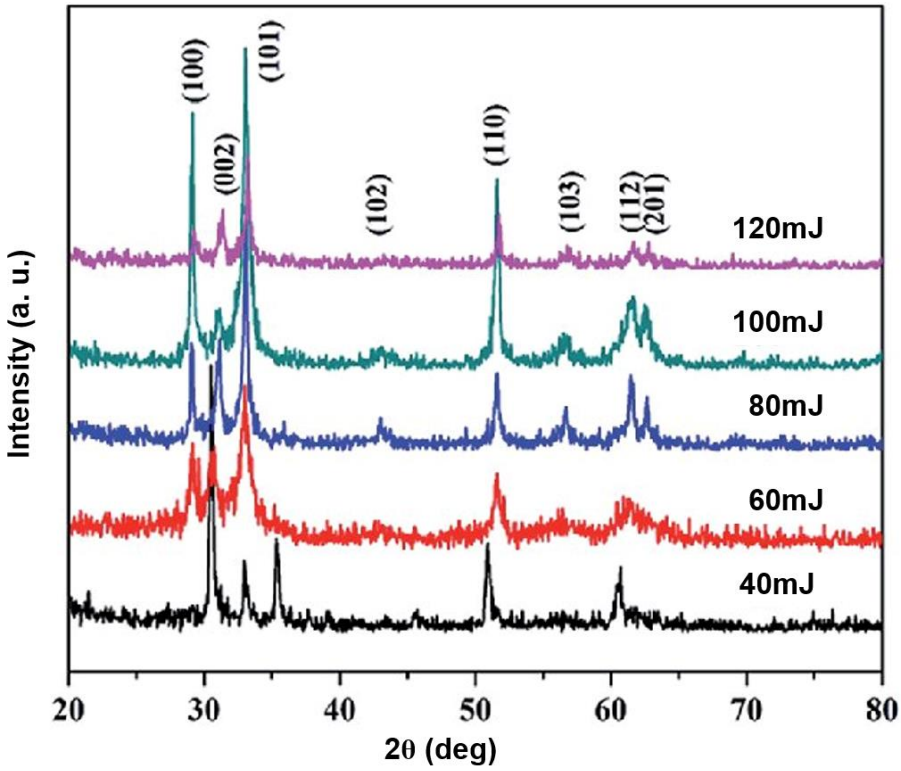

Fig. (3) The XRD patterns of the InN nanoparticles prepared in this work

Figure (4) shows the FE-SEM images of the InN nanoparticles prepared in this work at different laser energies. All samples show large aggregations, which is unavoidable in the nanoparticles prepared by methods and techniques including fluidic nature of the host medium as the prepared particles move freely and as a result of van der Waals forces, they aggregate to form reef-like structure. Using higher laser energy to prepare the InN nanoparticles has resulted in much more aggregations as can be seen in Fig. (4c,d). No indium clusters were observed in the surface morphology of the prepared samples, indicating a complete reaction of indium with nitrogen.

Figure (5) shows the FTIR spectra of the InN nanoparticles prepared in this work at different laser energies. All spectra are identical with some shift in the transmittance but the characteristic peaks corresponding to the vibration modes of the In-N bond can be seen in these spectra. The peak seen at 566 cm^{-1} is ascribed to the In-N stretching vibration, while the two peaks seen at 737 and 895 cm^{-1} are attributed to the In-N bending vibrations. The peak seen at 965 cm^{-1} is resulted from the In-N symmetric stretching vibration. Consequently, all functional groups constituting the indium nitride molecule were found in the prepared samples with no trace belonging to other materials, which reflects the high structural purity of the prepared nanoparticles.

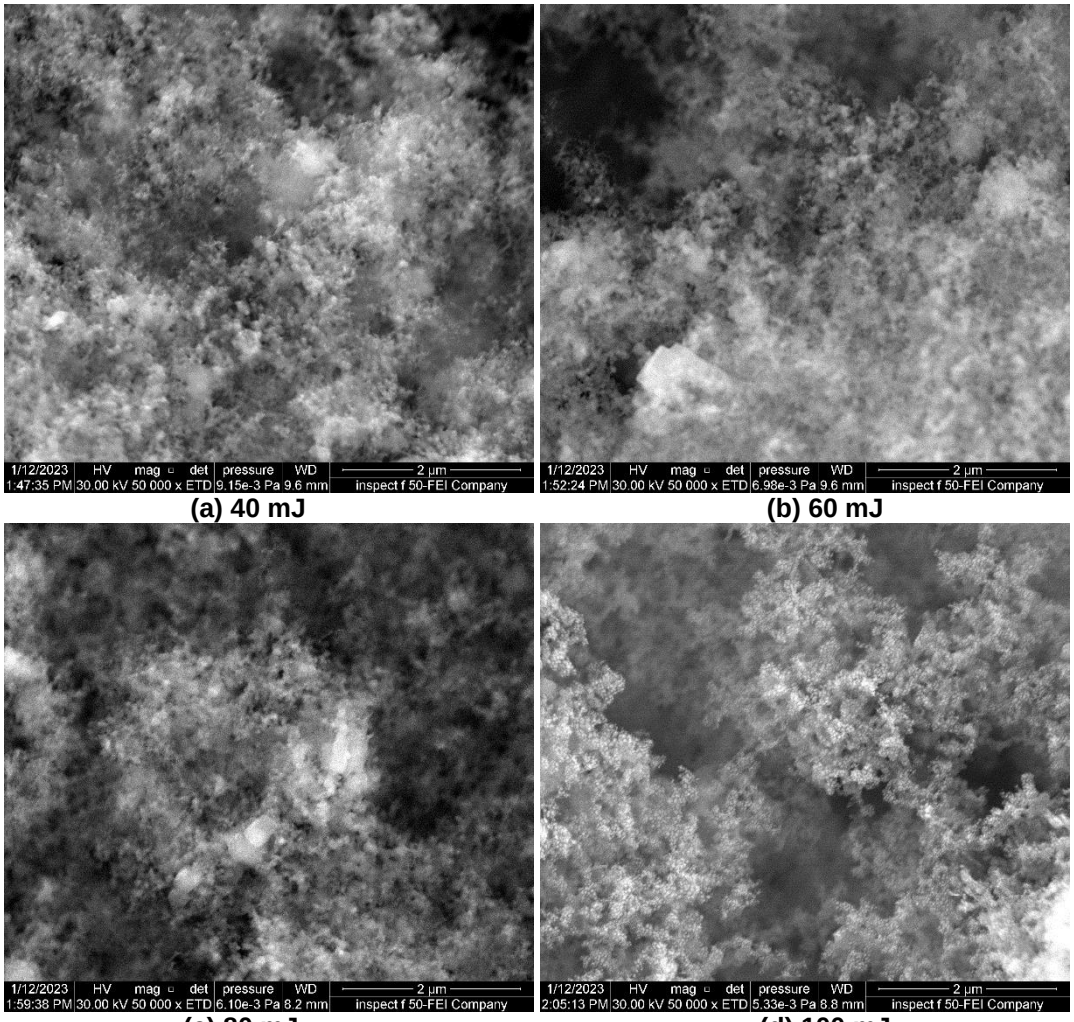

(a) 40 mJ **(b) 60 mJ**

(c) 80 mJ **(d) 100 mJ**

Fig. (4) The FE-SEM images of the InN nanoparticles prepared in this work using different laser energies

Figure (6) shows the UV-Visible absorption spectra of InN nanoparticles prepared in this work using different laser energies and constant ablation period of 10 minutes. These nanoparticles were immersed in suspensions in order to record their absorption spectra. In the UV region (200-400nm), the samples prepared using 100 and 120 mJ showed higher absorbance than other samples prepared using lower laser energies. In the visible region (400-700 nm), all samples approximately show comparable values of absorbance as the slight differences lie in the range 2-2.4. In the IR region (700-1000 nm), the behaviors of the prepared samples differ from each other again with smaller differences than were seen in the UV region. Accordingly, the absorbance of the prepared nanoparticles was found to depend on the laser energy used to prepare them, which determines the volume concentration of these nanoparticles, and hence the density of the solution to be measured.

4. Conclusion

In concluding remarks, indium nitride (InN) nanoparticles were prepared by pulsed laser ablation (PLAL) by irradiation of In target immersed in NH_4OH solution. The crystalline structure of the prepared nanoparticles was found to be wurtzite with tending to much more crystallization when higher laser energy is used in preparation process. The prepared InN nanoparticles show large aggregations to form reef-like structures. Using higher laser energy to prepare the InN nanoparticles has resulted in much more aggregations. No indium clusters were observed in the surface morphology of the prepared samples, indicating a complete reaction of indium with nitrogen. All functional groups constituting the indium nitride molecule were found in the prepared samples with no trace belonging to other materials, which reflects the high structural purity of the prepared nanoparticles. The absorbance of the prepared

nanoparticles was found to depend on the laser energy used to prepare them, which determines the volume concentration of these nanoparticles, and hence the density of the solution to be measured.

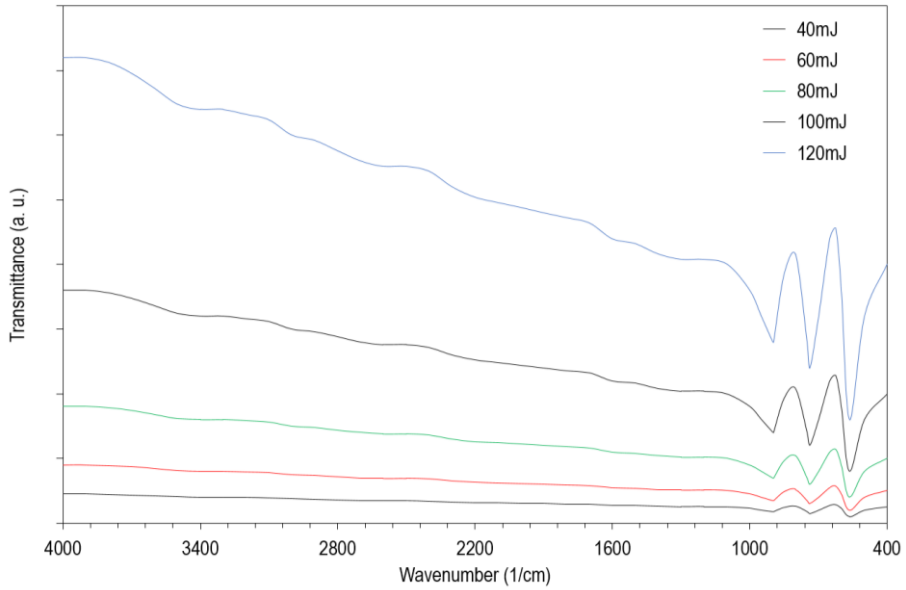

Fig. (5) The FTIR spectra of the InN nanoparticles prepared in this work using different laser energies

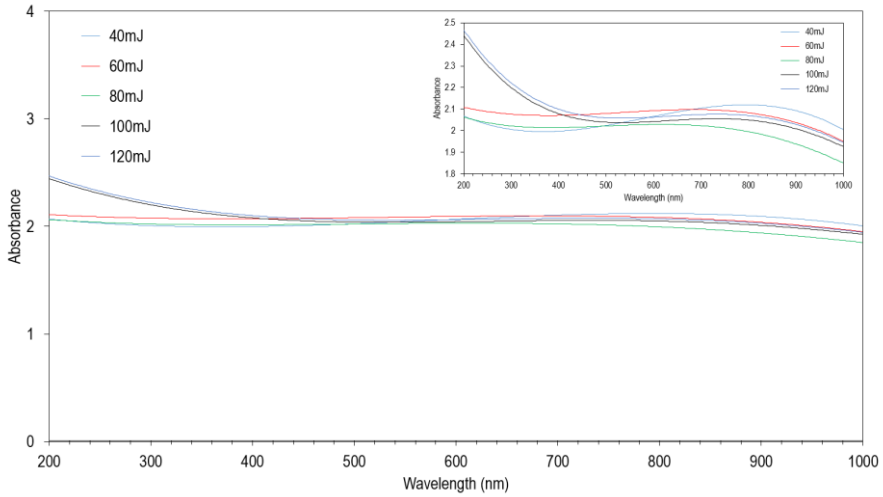

Fig. (6) The UV-visible spectra of the InN nanoparticles prepared in this work using different laser energies

Reference

[1] A. Tokarzewski and S. Podsiadlo, “Formation and thermal decomposition of Indium oxynitride compounds”, J. Therm. Anal. Calorim., 52 (1998) 481.
[2] A.G. Bhuiyan, A. Hashimoto and A. Yamamoto, “Indium nitride (InN): A review on growth, characterization, and properties”, J. Appl. Phys., 94 (2003) 2779.
[3] B. Umar et al., “Sputtered growth of high mobility InN thin films on different substrates using Cu-ZnO buffer layer”, Mater. Sci. Semicond. Process., 71 (2017) 166.
[4] D.G. Beck, “Method of epitaxially growing device structure with submicron group-III nitride layers uitlizing HVPE”, United States Patent, 2 (2003) 1.
[5] F.A. Mohammad, Y. Cao and L.M. Porter, “Characterization of Epitaxial Indium Nitride Interlayers for Ohmic Contacts to Silicon Carbide”, J. Electron. Mater., 36 (2007) 312–317.
[6] G.S. Smith and R.L. Snyder, “F N: A criteria for pattern evaluation”, J. Appl. Crystallogr., 12 (1979) 60–64.
[7] H. Sakakita et al., “Ammonia-free epitaxy of single-crystal InN using plasma-integrated gas-injection module”, Appl. Mater. Today, 27 (2022) 101489.
[8] O.A. Hammadi, M.K. Khalaf and F.J. Kadhim, “Silicon Nitride Nanostructures Prepared by Reactive Sputtering Using Closed-Field Unbalanced Dual Magnetrons”, Proc. IMechE, Part L, J. Mater.: Design & Appl., 231(5) (2017) 479-487.
[9] H.Z. Li et al., “Morphology and optical properties of RF sputtering deposited indium nitride layers under different N_2/Ar ratio”, J. Nanosci. Nanotechnol., 17 (2017) 524.

[10] I. Gorczyca et al., "Influence of indium clustering on the band structure of semiconducting ternary and quaternary nitride alloys", Phys. Rev. B, 80 (2009) 075202.
[11] I. Yonenaga et al., "Elastic properties of indium nitrides grown on sapphire substrates determined by nano-indentation", in comparison with other nitrides AIP Adv., 5 (2015) 077131.
[12] O.A. Hammadi, "Synthesis and Characterization of Polycrystalline Carbon Nitride Nanoparticles by Fast Glow Discharge-Induced Reaction of Methane and Ammonia", Adv. Sci. Eng. Med., 11(5) (2019) 346-350.
[13] B.K. Nasser and M.A. Hameed, "Narrow Emission Linewidth of Highly-Pure Silicon Nitride Nanoparticles in Different Dye Solutions as Random Gain Media", Nonl. Opt. Quantum. Opt., 53(1-2) (2019) 99-105.
[14] I.G. Pichugin and M. Tlachala, "X-ray analysis of indium nitride", Inorg. Mater., 14 (1978) 135–136.
[15] J. Wu et al., "Unusual properties of the fundamental band gap of InN", Appl. Phys. Lett., 80 (2002) 3967.
[16] J. Wu, "When group-III nitrides go infrared: New properties and perspectives", J. Appl. Phys., 106 (2009) 011101.
[17] K.P. Biju, A. Subrahmanyam and M.K. Jain, "Growth of InN Nanocrystalline Films by Activated Reactive Evaporation", J. Nanosci. Nanotech., 9 (2009) 1-6.
[18] K.P. Biju, A. Subrahmanyam and M.K. Jain, "Growth of InN thin films by modified activated reactive evaporation", J. Phys. D: Appl. Phys., 41 (2008) 155409.
[19] K.S.A. Butcher et al., "Nitrogen-rich indium nitride", J. Appl. Phys., 95 (2004) 6124.
[20] L. Braic and N.C. Zoita, "Influence of the deposition time and temperature on the texture of InN thin films grown by RF-magnetron sputtering", Optoelectron. Adv. Mater. Rapid Commun., 4 (2013) 2013.
[21] M. Amirhoseiny et al., "Characterizations of InN thin films grown on Si (110) substrate by reactive sputtering", J. Nanomater., 11 (2011) 1.
[22] F.J. Kadhim and A.A. Anber, "Fabrication of Nanostructured Silicon Nitride Thin Film Gas Sensors by Reactive DC Magnetron Sputtering", Proc. IMechE, Part N, J. Nanomater. Nanoeng. Nanosys., 231(4) (2017) 173-178.
[23] D.A. Taher and M.A. Hameed, "Spectroscopic Characteristics of Silicon Nitride Thin Films Prepared by DC Reactive Sputtering Using Silicon targets with Different Types of Conductivity", Iraqi J. Appl. Phys., 19(4A) (2023) 73-76.
[24] M. Amirhoseiny, Z. Hassan and S.S. Ng, "Comparative study on structural and optical properties of nitrogen rich InN on Si (110) and 6H-SiC", Surf. Eng., 29 (2013) 561.
[25] M. Amirhoseiny, Z. Hassan and S.S. Ng, "Growth of InN thin films on different Si substrates at ambient temperature", Microelectron. Int., 30 (2013) 63.
[26] N.C. Zoita et al., "InN thin films deposited on flexible substrates by reactive RF-magnetron sputtering", Optoelectron. Adv. Mater. Rapid Commun., 2 (2008) 719.
[27] O.A. Hammadi, "Using third-harmonic radiation of Nd:YAG laser to fabricate high-quality microchannels for biomedical applications", Optik, 208 (2020) 164147.
[28] S. Krukowski et al., "Thermal properties of indium nitride", J. Phys. Chem. Solids, 59 (1998) 289–295.
[29] S. Ruffenach et al., "Recent advances in the MOVPE growth of indium nitride", phys. stat. sol., 18 (2010) 9.
[30] S.A. Osman, S.S. Ng and Z. Hassan, "Reactive Sputtering Growth of Indium Nitride Thin Films on Flexible Substrate under Different Substrate Temperatures", J. Phys.: Conf. Ser., 1535 (2020) 012029.
[31] S.C. Jain et al., "III–nitrides: Growth, characterization, and properties", J. Appl. Phys., 87 (2000) 965.
[32] T. Tansley and C.P. Foley, "Electron mobility in indium nitride", Electron. Lett., 20 (1984) 1066.
[33] T.L. Tansley, "Crystal structure, mechanical properties, thermal properties and refractive index of InN", in Properties of Group III Nitrides, EMIS Datareviews Series, edited by J.H. Edgar (British Institution of Electrical Engineers Publ., INSPEC) (1994), p. 35.
[34] W. Gotz et al., "Hall-effect characterization of III-V nitride semiconductors for high efficiency light emitting diodes", Mater. Sci. Eng. B, 59 (1991) 211.
[35] W. Paszkowicz et al., "Lattice parameters, density and thermal expansion of InN microcrystals grown by the reaction of nitrogen plasma with liquid indium", Philos. Mag., 79 (1999) 1145–1154.
[36] Y. Hao and J.C. Zhang, "Nitride wide bandgap semiconductor material and electronic devices", CRC Press (Boca Raton, 2017).
[37] Y. Nanishi, Y. Saito and T. Yamaguchi, "RF-molecular beam epitaxy growth and properties of InN and related alloys", Japanese J. Appl. Phys., 42 (2003) 2549.
[38] G.B. Damas et al., " Understanding indium nitride thin film growth under ALD conditions by atomic scale modelling: From the bulk to the In-rich layer", Appl. Surf. Sci., 592 (2022) 153290.
[39] Y.S. Lu et al., "An investigation of the Young's modulus of single-crystalline wurtzite indium nitride using an atomic force microscopy based micromechanical bending test", Appl. Phys. Lett., 101 (2012) 221906.
[40] Y.Z. Bai et al., "Preparation of InN nanocrystals by solvo-thermal method", J. Cryst. Growth, 241 (2002) 189.
[41] Z.Y. Lee et al., "Radio-frequency sputtering growth of indium nitride thin film on flexible substrate", Mater. Sci. Forum., 846 (2016) 650.
[42] O.A. Hammadi, M.K. Khalaf and F.J. Kadhim, "Fabrication and Characterization of UV Photodetectors Based on Silicon Nitride Nanostructures Prepared by Magnetron Sputtering", Proc. IMechE, Part N, J. Nanomater. Nanoeng. Nanosys., 230(1) (2016) 32-36.
[43] F.J. Kadhim and A.A. Anber, "Highly-Pure Nanostructured Silicon Nitride Films Prepared by Reactive DC Magnetron Sputtering", J. Indust. Eng. Sci., 25(5) (2016) 91-94.
[44] B.K. Nasser and M.A. Hameed, "Structural Characteristics of Silicon Nitride Nanostructures Synthesized by DC Reactive Magnetron Sputtering", Iraqi J. Appl. Phys., 15(4) (2019) 33-36.
[45] M. Lei et al., "Synthesis of N-deficient indium nitride nanowires and their room-temperature ferromagnetism", Mater. Lett., 73 (2012) 166-168.
[46] W.Z. Shen et al., "Critical point transitions of wurtzite indium nitride", Solid State Commun., 137(1-2) (2006) 49-52.
[47] J.T-Thienprasert et al., "X-ray absorption spectroscopy of indium nitride, indium oxide, and their alloys", Comput. Mater. Sci., 49(1) (2010) S37-S42.
[48] H.S. Lee, S.S. Ng and F.K. Yam, "Sol–gel spin coating growth of magnesium-doped indium nitride thin films", Vacuum, 155 (2018) 16-22.
[49] W.-S. Jung, O.H. Han and S.-A. Chae, "Characterization of wurtzite indium nitride synthesized from indium oxide by In-115 MAS NMR spectroscopy", Mater. Lett., 61(16) (2007) 3413-3415.

[50] D.K. Nguyen et al., “First-principles study of indium nitride monolayers doped with alkaline earth metals”, RSC Adv., 13(48) (2023) 33634-33643.
[51] C.C. Loo et al., “Probing the charge state of threading dislocations in indium nitride through advanced atomic force microscopy”, Mater. Characteriz., 205 (2023) 113279.
[52] O.A. Hammadi, “New Technique to Synthesize Silicon Nitride Nanopowder by Discharge-Assisted Reaction of Silane and Ammonia”, Mater. Res. Exp., 8(8) (2021) 085013.
[53] D.A. Taher and M.A. Hameed, “Structural and Hardness Characteristics of Silicon Nitride Thin Films Deposited on Metallic Substrates by DC Reactive Sputtering Technique”, Silicon, 15 (2023) 7855-7864.
[54] F. Peng et al., “First-principles calculations on structure and elasticity of wurtzite-type indium nitride under pressure”, J. Alloys Comp., 475(1-2) (2009) 885-888.
[55] T. Lindgren, M. Larsson and S.-E. Lindquist, “Photoelectrochemical characterisation of indium nitride and tin nitride in aqueous solution”, Sol. Ener. Mater. Solar Cells, 73(4) (2002) 377-389.
[56] Q. Guo et al., “Optical constants of indium nitride”, Solid State Commun., 83(9) (1992) 721-723.
[57] S. Krukowski et al., “Thermal properties of indium nitride”, J. Phys. Chem. Solids, 59(3) (1998) 289-295.
[58] F.J. Kadhim, O.A. Hammadi and A.A. Anber, “Spectroscopic Study of Chromium-Doped Silicon Nitride Nanostructures Prepared by DC Reactive Magnetron Sputtering”, Iraqi J. Appl. Phys., 17(2) (2021) 9-12.
[59] Z.H Lan et al., “Growth mechanism, structure and IR photoluminescence studies of indium nitride nanorods”, J. Cryst. Growth, 269(1) (2004) 87-94.
[60] H. Timmers, S.K. Shrestha and A.P. Byrne, “The potential of ion beam techniques for the development of indium nitride”, J. Cryst. Growth, 269(1) (2004) 50-58.
[61] C. Meissner et al., “Indium nitride quantum dot growth modes in metalorganic vapour phase epitaxy”, J. Cryst. Growth, 310(23) (2008) 4959-4962.
[62] J.A.S. Laranjeira et al., “Novel buckled graphenylene-like InN and its strain engineering effects”, Comput. Theor. Chem., 1231 (2024) 114418.

